

Field Measurement of a Fermilab-Built Full Scale Prototype Quadrupole Magnet for the LHC Interaction Regions

R. Bossert, R. Carcagno, J. DiMarco, S. Feher, H. Glass, J. Kerby, M. J. Lamm, A. Nobrega, T. Nicol, T. Ogitsu, D. Orris, T. Page, R. Rabehl, G. Sabbi, P. Schlabach, J. Strait, C. Sylvester, M. Tartaglia, J. C. Tompkins, G. Velev, and A. V. Zlobin

Abstract—Superconducting low-beta quadrupole magnets for the interaction regions of the Large Hadron Collider have been developed by the US-LHC Accelerator Project. These 70 mm bore 5.5 m long quadrupoles are intended to operate in superfluid helium at 1.9 K with a nominal field gradient of 215 T/m. Following a series of 2 m long models, a full scale cryostated cold mass has been fabricated and cold tested at Fermilab. Magnetic field measurements of the prototype, including determination of the field axis using a single stretched wire, have been performed. These measurements and comparisons with results from the model magnets as well as field quality and alignment requirements are reported in this paper.

Index Terms—Magnetic fields, quadrupole, superconductivity.

I. INTRODUCTION

TO ACHIEVE a luminosity of $10^{34} \text{ cm}^{-2}\text{s}^{-1}$ at the LHC, special quadrupole magnets are required for the final focusing triplets in the interaction region [1]. These magnets must provide a field gradient of 215 T/m over a 70 mm bore with good field quality due to large and rapidly varying values of the β -function in the interaction region. Half of these inner triplet quadrupoles (MQXB) will be built at Fermilab. The other half will be built at KEK. A short model magnet program to validate the design of the MQXB and construction techniques was completed last year.¹ A full scale prototype (MQXP01) of an MQXB cold mass was recently constructed and tested. During testing, an extensive program of field harmonics measurements was executed. In this paper we present results of the measurements and compare them with expectations from the magnet design as well as measurements made of the 2 m model magnets. In addition to field quality measurements, alignment of the cold mass relative

to the cryostat was measured repeatedly both warm and cold. Results from these studies are also reported.

II. MAGNET DESIGN

The MQXB design, developed by a Fermilab-LBNL collaboration, is based on four two-layer coils connected in series, surrounded by stainless steel collar and iron yoke laminations. The prototype cold mass has the same cross-section and end design as that of the last 4 models constructed. Details of the design evolution and improvements in field quality during the course of the model magnet program can be found in [2].

III. FIELD HARMONICS MEASUREMENT SYSTEM

Magnetic measurements presented in this paper were performed using a variety of rotating coils. Probes used have a tangential winding for measurement of higher order harmonics as well as dedicated dipole and quadrupole windings sensitive to the lowest order components of the field. These windings also allow for bucking the large dipole and quadrupole components in the tangential winding signal. Most measurements presented in this paper were made with a 3 section integral coil of 41 mm nominal diameter and overall length 7.1 m. The active length of each section as well as the interconnection region between sections is an integral multiple of the 0.114 m cable winding pitch length of the MQXB magnet. Warm measurements made for quality control during magnet production were taken with a 25 mm radius coil of 1 m length with an integrated drive system ("mole").

The readout system of the mole was described in [2]. A new readout system for the integral probe has been constructed. Coil winding voltages are read using METROLAB PDI integrators. One integrator is required for each winding of the probe. Windings in the separate sections are connected in series. An HP 3458 DVM is used to monitor magnet current. Integrators and DVM are triggered simultaneously by an angular encoder on the probe shaft, synchronizing measurements of field and current. Feed down of the quadrupole signal to the dipole is used to center the probe in the magnet. A horizontal drive system allows for longitudinal scans of the magnet.

Manuscript received September 24, 2001. This work was supported by the U.S. Department of Energy.

R. Bossert, R. Carcagno, J. DiMarco, S. Feher, H. Glass, J. Kerby, M. J. Lamm, A. Nobrega, T. Nicol, D. Orris, T. Page, R. Rabehl, P. Schlabach, J. Strait, C. Sylvester, M. Tartaglia, J. C. Tompkins, G. Velev, and A. V. Zlobin are with Fermilab, Batavia, IL 60510 USA (e-mail: schlabach@fnal.gov).

G. Sabbi is with Lawrence Berkeley National Laboratory, Berkeley, CA, USA.

T. Ogitsu is with KEK, Tsukuba, Japan.

Publisher Item Identifier S 1051-8223(02)03470-X.

¹Nine 2 m models were built (HGQ01-09). Eight were tested in superfluid helium at the Fermilab Vertical Magnet Test Facility.

TABLE I
MEASURED HARMONICS OF THE MAGNET AT 6 kA

| n | HGQ | | | | | MQXP | |
|----------|-------|-------|-------|-------|-------|-------|--|
| | 05 | 06 | 07 | 08 | 09 | 01 | |
| b_3 | 0.72 | 0.25 | 0.18 | 0.61 | 0.71 | 0.28 | |
| b_4 | 0.00 | 0.09 | 0.01 | -0.12 | -0.05 | -0.44 | |
| b_5 | -0.04 | -0.11 | -0.04 | -0.01 | 0.08 | 0.04 | |
| b_6 | -0.30 | -0.05 | -0.45 | -0.06 | -0.28 | -0.55 | |
| b_7 | 0.01 | -0.03 | 0.02 | -0.01 | 0.06 | 0.00 | |
| b_8 | 0.00 | 0.00 | 0.00 | 0.00 | -0.01 | -0.02 | |
| b_9 | 0.00 | 0.00 | -0.01 | 0.00 | 0.00 | 0.04 | |
| b_{10} | 0.01 | 0.00 | -0.02 | -0.01 | -0.01 | 0.00 | |
| a_3 | 0.12 | -0.27 | 0.41 | -0.01 | 0.35 | -0.02 | |
| a_4 | 0.19 | -0.31 | -0.50 | -0.43 | 0.31 | 1.03 | |
| a_5 | 0.05 | -0.07 | -0.24 | 0.12 | -0.14 | -0.52 | |
| a_6 | -0.03 | -0.05 | -0.10 | -0.03 | 0.04 | -0.01 | |
| a_7 | 0.01 | 0.00 | 0.07 | 0.00 | 0.02 | 0.03 | |
| a_8 | 0.00 | 0.00 | 0.01 | -0.01 | 0.01 | -0.03 | |
| a_9 | 0.00 | 0.00 | 0.01 | -0.01 | 0.00 | 0.02 | |
| a_{10} | 0.00 | 0.00 | 0.00 | 0.00 | 0.00 | 0.01 | |

IV. FIELD QUALITY ANALYSIS

In the straight section of the magnet, the field is represented in terms of harmonic coefficients defined by the power series expansion

$$B_y + iB_x = B_2 10^{-4} \sum_{n=1}^{\infty} (b_n + ia_n) \left(\frac{x + iy}{r_0} \right)^{n-1} \quad (1)$$

where B_x and B_y are the transverse field components, B_2 is the quadrupole field strength, b_n and a_n are the $2n$ -pole coefficients ($b_2 = 10^4$) at the LHC reference radius r_0 of 17 mm.² The coordinate system for magnetic measurement is defined in [3].

Improvement in coil production techniques led to steady improvement in field quality in the first few model magnets [2]. Field harmonics in the last 5 magnets of the series were consistently small. The 5.5 m coils for the MQXP01 were produced with new tooling. Based on experience with the short models, one might expect larger harmonics in the first few magnets. Table I shows the measured harmonics up to the 20-pole for the last 5 model magnets and the MQXP01. The largest harmonic is 1 unit of skew octupole, much smaller than the several units of low order harmonics seen in the first few model magnets. Similar examples of 0.5 to 1 unit of low order harmonics were observed in the later model magnets. Note that the comparison given is between measurements in the straight section of the model magnets and integral measurements of the prototype magnet. The integral b_6 is thus 0.2 units less negative than that of the body due to the large systematic normal dodecapole in the lead end. The effect of other systematic harmonics in the ends is less than 0.01 unit.

While field quality of the prototype is quite comparable to that of the later model magnets, it would have been even better were it not for a local distortion in the field. Quality assurance measurements of the warm MQXP01 taken after collaring the magnet and again after it was yoked and skinned indicated that a relatively large (a few units of most lower order harmonics) distortion of the field at a particular longitudinal location in

TABLE II
REFERENCE HARMONICS AT COLLISION FOR THE MQXB (V3.2)

| n | $\langle b_n \rangle$ | $d(b_n)$ | $\sigma(b_n)$ | $\langle a_n \rangle$ | $d(a_n)$ | $\sigma(a_n)$ |
|--------------------------------------|-----------------------|----------|---------------|-----------------------|----------|---------------|
| Straight section (L_{mag} 4.76 m) | | | | | | |
| 3 | 0 | 0.60 | 0.27 | 0 | 0.23 | 0.27 |
| 4 | 0 | 0.15 | 0.27 | 0 | 0.20 | 0.27 |
| 5 | 0 | 0.15 | 0.10 | 0 | 0.15 | 0.10 |
| 6 | 0 | 0.45 | 0.20 | 0 | 0.07 | 0.03 |
| 7 | 0 | 0.04 | 0.02 | 0 | 0.03 | 0.02 |
| 8 | 0 | 0.01 | 0.02 | 0 | 0.01 | 0.01 |
| 9 | 0 | 0.01 | 0.01 | 0 | 0.01 | 0.01 |
| 10 | 0 | 0.01 | 0.01 | 0 | 0.01 | 0.01 |
| Lead end (L_{mag} 0.41 m) | | | | | | |
| 3 | 0 | 0.90 | 0.80 | 0 | 0.90 | 0.80 |
| 4 | 0 | 0.70 | 0.80 | 0 | 0.70 | 0.80 |
| 5 | 0 | 0.40 | 0.50 | 0 | 0.40 | 0.50 |
| 6 | 3.10 | 0.20 | 0.07 | -0.35 | 0.20 | 0.07 |
| 7 | 0 | 0.10 | 0.04 | 0 | 0.10 | 0.04 |
| 8 | 0 | 0.03 | 0.03 | 0 | 0.03 | 0.03 |
| 9 | 0 | 0.01 | 0.01 | 0 | 0.01 | 0.01 |
| 10 | -0.05 | 0.01 | 0.01 | 0 | 0.01 | 0.01 |
| Return end (L_{mag} 0.33 m) | | | | | | |
| 3 | 0 | 0.90 | 0.80 | 0 | 0.90 | 0.80 |
| 4 | 0 | 0.70 | 0.80 | 0 | 0.70 | 0.80 |
| 5 | 0 | 0.40 | 0.50 | 0 | 0.40 | 0.50 |
| 6 | -0.4 | 0.30 | 0.07 | 0 | 0.20 | 0.07 |
| 7 | 0 | 0.10 | 0.04 | 0 | 0.10 | 0.04 |
| 8 | 0 | 0.03 | 0.03 | 0 | 0.03 | 0.03 |
| 9 | 0 | 0.01 | 0.01 | 0 | 0.01 | 0.01 |
| 10 | -0.05 | 0.05 | 0.01 | 0 | 0.01 | 0.01 |

the cold mass was introduced between the two sets of measurements. Subsequent inspection of the magnet found an approximately 1 mm deviation in straightness in the weld joining the two halves of the skin in the region where the distortion was seen. Measurements of the magnet made cold show similar features. Changes in procedure during construction of the production magnets should eliminate this source of field error.

Given in Table II are the set of reference harmonics for MQXB magnets. These reference harmonics were developed based on models HGQ05-09 (Table I). Reference harmonics in the magnet ends were based on the last 4 magnets which had the final end design. For each harmonic component, values of the mean, uncertainty in mean and standard deviation are listed separately for magnet body and ends. As a figure of merit for comparing the harmonics of the prototype magnet to the reference table, we construct an "error band" for each harmonic as $\langle b_n \rangle \pm [d(b_n) + 3\sigma(b_n)]$ or $\langle a_n \rangle \pm [d(a_n) + 3\sigma(a_n)]$. Reference harmonics for the body and end are weighted to determine an error band appropriate for comparison to the integral field of the prototype. Fig. 1 shows the measured harmonics of the MQXP01 relative to this error band. All harmonics are within the 3σ limit. Note that we are not defining this error band as an acceptance criteria for production magnets. However, some such mechanism is likely to be and has been used during production of other magnet series. For example, 2 and 3σ bands were used during production of Fermilab Main Injector dipoles with appropriate courses of action defined for each band [4].

Large differences between harmonics measured during up and down ramp increasing with increasing ramp rate were observed for several of the later model magnets (HGQ06-08) [2], [3]. This effect was found to be due to eddy currents in the

²Field harmonics in all tables are given in these units of 10^{-4} normalized to the main field.

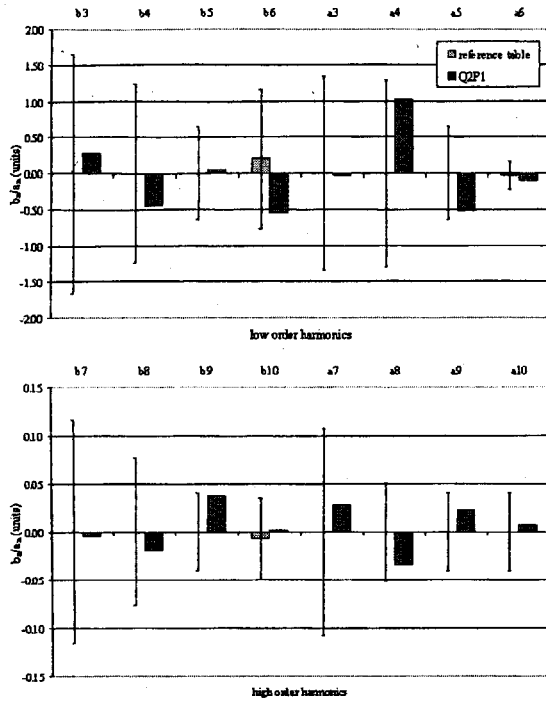


Fig. 1. Comparison of the field quality of the MQXP01 with reference harmonics.

TABLE III
DIFFERENCE BETWEEN FIELD HARMONICS MEASURED ON THE UP AND DOWN RAMP AT DIFFERENT RAMP RATES (6 kA)

| magnet | Δb_6 | | |
|--------|--------------|--------|--------|
| | 10 A/s | 40 A/s | 80 A/s |
| HGQ06 | 0.20 | 1.05 | 2.07 |
| HGQ07 | 0.05 | 0.55 | 1.10 |
| HGQ08 | 0.10 | 0.72 | 1.46 |
| HGQ09 | -0.12 | -0.13 | -0.14 |
| MQXP01 | -0.11 | -0.18 | -0.25 |

magnet cable caused by low crossover resistance induced by a change in coil curing cycle. Coils for MQXP01 were cured using the modified curing cycle introduced during production of the last model magnet. The difference between up and down ramp normal dodecapole as a function of ramp rate for HGQ06-09 and the prototype is given in Table III. Cable eddy current effects are small in both HGQ09 and the prototype.

A comparison of measured harmonics in the magnet lead end is given in Table IV for HGQ06-9 and the MQXP01. Calculations of the harmonics are also given. As in the magnet straight section, the multipole components in the end regions are expressed in units of 10^{-4} of the quadrupole field.³ Measurements in the lead end of the 5 magnets are quite consistent and agree well with calculations. The measured b_6 is 0.4 to 0.5 units lower than the predicted value. This discrepancy is believed to be due to local shims in the magnet end region not included in the calculation.

³The magnetic length L_m of the end region is defined as the length of straight section which would provide an equivalent integrated gradient and defines the appropriate weighting factor for end and body harmonics in the integral field of the magnet.

TABLE IV
CALCULATED AND MEASURED HARMONICS OF THE MAGNET LEAD END

| harmonic | calc. | HGQ | | | | MQXP | |
|----------|-------|------|------|------|------|------|--|
| | | 06 | 07 | 08 | 09 | 01 | |
| b_6 | 3.5 | 3.1 | 3.1 | 3.1 | 3.0 | 3.1 | |
| b_{10} | -0.1 | -0.1 | -0.1 | -0.0 | -0.1 | -0.1 | |
| a_6 | -0.7 | -0.4 | -0.3 | -0.4 | -0.4 | -0.5 | |
| a_{10} | 0.0 | 0.0 | 0.0 | 0.0 | 0.0 | 0.0 | |

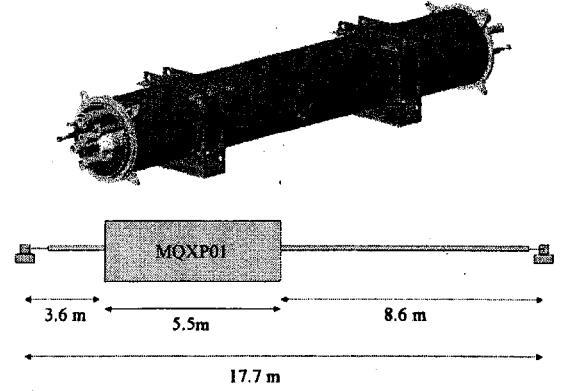


Fig. 2. Top: magnet cryostat. Fiducial holders can be seen at the corners of the magnet support structure. Bottom: schematic of the magnet and stretched wire system during alignment.

Injection takes place at fields (B_z) in the MQXB ranging from 12.3 to 14.1 T/m due to the different β^* in the different interaction regions. At these low levels of excitation (670 to 770 A), persistent currents result in an additional component of the allowed harmonics. Averaged over the model magnet series, the additional b_6 at 770 A (670 A) is -1.2 (-1.6) units with an RMS of 0.5 (0.6). Measurements of b_6 in the MQXP01 give values in the same range: -0.76 (770 A) and -0.83 (670 A).

V. ALIGNMENT OF THE MQXB

Alignment of the MQXA and MQXB cold masses relative to the beamline directly effects luminosity as they are nearest the interaction point, have large gradients and are in the region where the beam experiences the largest beta function. Requirements for placement of the cold mass relative to the cryostat during assembly as well as requirements for measurement of the magnetic axis and roll angle of the field relative to fiducial elements mounted on the cryostat have been studied [6]. An additional issue is warm-cold correlation in alignment. With respect to measurement on the test stand, an error budget of 0.18 mm, 0.25 mm, and 0.1 mrad has been assigned for determination of the average field center, the true axis, and the roll angle respectively. These uncertainties include the contribution due to survey.

The cryostated prototype is shown in Fig. 2. Alignment of the cold mass in the cryostat was accomplished mechanically. A reference line corresponding to the origin of the field coordinate system averaged along the length was scribed on the magnet. Lugs were then welded to the cold mass along this line. The cold mass was then slid into the cryostat where the lugs engage features on magnet supports in the cryostat [7]. Magnetic field

measurements of the magnet axis and roll angle relative to the cryostat were performed only after assembly of the cold mass in the cryostat, in fact, after installation of the magnet on the cold test stand.

Alignment measurements of the prototype magnet were performed with a single stretched wire system (SSW). Details of the SSW system and the measurement techniques involved are summarized in [8].

VI. ALIGNMENT OF THE MQXP01

A schematic of the magnet and SSW system is shown in Fig. 2. The full-length MQXA/MQXB anti-cryostat is used, so that measurement constraints and geometry correspond to those present during testing of production MQXBs, which have two cold masses in one cryostat.

One of the primary concerns with stretched wire alignment is correction for effects of sag—about 3 mm for the 17.7 m wire. Repeated measurements indicate that the possible systematic uncertainty in the measured vertical offset due to sag removal is less than 0.03 mm. Effects stemming from slight magnetic susceptibility of the long wire at high fields were observed. Their influence on alignment results is small or compensated for during sag calibration.

Repeated measurements of the magnetic center both warm and cold were made over the course of several months. Variation of the measured average field center in horizontal and vertical directions is approximately 0.03 mm. Reproducibility of the measured center offset at the magnet ends (the true magnetic axis) is 0.08 mm. These results include transfer of stretched wire position to cryostat fiducials using a laser tracker. No evidence was seen for motion of the cold mass in the cryostat other than a 0.2 mm lowering of the vertical center when the magnet is cooled. A mechanical model of the cold mass and cryostat predicted a 0.16 mm shift upward. The difference is consistent with uncertainty in material properties used in the analysis. All measurements (warm and cold) were done with the magnet under vacuum. Offsets of a few hundred microns were found during vacuum pump-down.⁴

Field angle measurements with respect to gravity were performed warm and cold during each test cycle. The relative angle of the magnet cold-mass with respect to the cryostat was 0.8 mrad, much smaller than the ± 10 mrad precision needed during assembly. Uncertainty of the roll angle measurement was 0.03 mrad. Changes in roll angle at the level of 0.1–0.2 mrad with respect to gravity were observed during the course of these tests (a period of several months). Table V shows these

TABLE V
MEASURED CHANGES IN ROLL ANGLE AND CRYOSTAT ANGLE RELATIVE TO THE FIRST MEASUREMENT. ANGLES ARE GIVEN IN mrad; MEASUREMENT UNCERTAINTY IS 0.05 mrad

| roll change | magnet | cryostat |
|-----------------|--------|----------|
| cold, TC1 | -0.12 | -0.09 |
| warm, after TC1 | -0.16 | -0.26 |
| warm, after TC2 | -0.27 | -0.24 |
| cold, TC3 | -0.26 | -0.28 |
| warm, after TC3 | -0.04 | -0.18 |

changes in the roll angle as well as changes in the angle of the cryostat. Roll angle changes seem to be correlated with cryostat motion (i.e., the entire magnet assembly is moving), perhaps associated with motion during application of vacuum, and/or motion of the test stand or building under floor loading or seasonal conditions. This will be monitored more closely during production measurements.

VII. CONCLUSIONS

A full length prototype of MQXB magnets for the LHC interaction region has been constructed and tested. Integral and end field harmonics of the prototype are quite small and consistent with those measured in later magnets in the short models of this design. Cable eddy current effects are small. The effect of the magnetization on the field is similar to that seen in previous models. Field alignment measurements show that the placement of the cold mass in the cryostat without field measurement was much better than required. Uncertainties of the field alignment with respect to fiducials on the cryostat were also smaller than allowed for in the measurement error budget.

REFERENCES

- [1] "LHC conceptual design," CERN AC/95-05 (LHC).
- [2] N. Andreev *et al.*, "Field quality in Fermilab-built models of quadrupole magnets for the LHC interaction region," *IEEE Trans. Appl. Supercond.*, vol. 11, no. 1, Mar. 2001.
- [3] N. Andreev *et al.*, "Field quality in Fermilab-built models of high gradient quadrupole magnets for the LHC interaction regions," *IEEE Trans. Appl. Supercond.*, vol. 10, no. 1, Mar. 2000.
- [4] C. S. Mishra, "Main injector dipole magnet acceptance criteria," Fermilab Internal Note MI-0130, Feb. 1995.
- [5] N. Andreev *et al.*, "Field quality of quadrupole R&D models for the LHC IR," in *1999 Particle Accelerator Conf.*, New York, Apr. 1999.
- [6] T. Sen, "Alignment tolerances of IR quadrupoles in the LHC," in LHC IR Alignment Workshop, Fermilab, Oct. 1999, FER-MILAB-CONF-99-304.
- [7] T. H. Nicol, C. Darve, Y. Huang, and T. M. Page, "LHC interaction region quadrupole cryostat design and fabrication," submitted for publication.
- [8] J. DiMarco *et al.*, "Field alignment of quadrupole magnets for the LHC interaction regions," *IEEE Trans. Appl. Supercond.*, vol. 10, no. 1, Mar. 2000.

⁴We note that production fiducials were not available for the prototype and temporary ones were used. These were welded at the approximate positions of the production fiducials and may contribute to measurement uncertainty.